

Global Particle Balance of Long Duration Discharges on TRIAM-1M

SAKAMOTO Mizuki and TRIAM Group

*Advanced Fusion Research Center, Research Institute for Applied Mechanics,
Kyushu University, Fukuoka 816-8580, Japan*

(Received: 18 December 2001 / Accepted: 15 May 2002)

Abstract

In the superconducting tokamak TRIAM-1M, the ultra-long discharge of the duration of 3 h 10 min was achieved. In this discharge, the net wall pumping rate became zero (i.e. apparent wall saturation) around $t \sim 30$ min and after that the plasma was sustained without fueling until the end of the discharge. The wall plays a role of the particle sink for the first 30 min and afterwards plays a role of the particle source. The averaged wall pumping rate before the apparent wall saturation is evaluated to be about 2.4×10^{16} atoms $\text{m}^{-2} \text{s}^{-1}$ and that after the wall saturation is about -8×10^{15} atoms $\text{m}^{-2} \text{s}^{-1}$. The total amount of wall-pumped hydrogen atoms was finally released from the wall until the end of the discharge. One candidate of the causes of the apparent wall saturation is the increase in hydrogen release from the vacuum vessel due to the temperature increase.

Keywords:

particle balance, wall recycling, wall pumping, tokamak, ultra-long discharge

1. Introduction

The achievement of stable long pulse operation is one of the requirements for the future fusion reactors. In TRIAM-1M, the study and development of long pulse operation have intensively been carried out [1-6]. In order to keep the steady state toroidal magnetic field, the Nb₃Sn superconducting magnet system was successfully developed [1]. The lower hybrid current drive system, the position and fueling control systems have also been developed and the ultra-long discharges have been achieved [2-4]. Recently, ultra-long discharges with the duration longer than 3 hours (i.e. a new record) were achieved [7].

In order to achieve the stable steady state operation, understanding of the wall property during the long duration discharge is indispensable. It was observed that the density control was lost in the final phase of the long duration discharge due to the increase in the out-flux

from the wall in JET [8], Tore Supra [9] and TRIAM-1M [10]. The wall conditions continue to change with time during the discharge. For example, strong radiation damage, which provides a new particle-trap area, occurs during the discharge [11]. It is reported that co-deposition of in-vessel elements, so called "tokamakium", also occurs during the discharge [12,13]. The co-deposited material of Mo with O can retain one order larger amount of hydrogen than that of the normal Mo [11,13]. The temperature of the first wall increases during the discharge. The temperature increase causes out-gassing from the wall.

In the longest discharge with the duration of 3 h 10 min, the density control was lost after $t \sim 30$ min and the plasma density was sustained by the recycling particles alone. In this article, the wall property of the longest discharge is investigated via the global particle balance

Corresponding author's e-mail: sakamoto@triam.kyushu-u.ac.jp

in the vacuum vessel. In Sec. 2, TRIAM-1M device and the long tokamak operation are presented. The global particle balance of the longest discharge are presented and discussed in Sec. 3. Finally, a summary is given in Sec. 4.

2. Experimental Setup and the Long Tokamak Operation

Figure 1 shows a bird's-eye view of TRIAM-1M. Sixteen superconducting toroidal field coils, which are made of Nb₃Sn, are installed. Toroidal magnetic field is up to 8 T. The plasma vacuum vessel has a D-shaped cross-section with the horizontal length of 0.26 m and the vertical length of 0.38 m. The poloidal field coils, which are made of normal conductor Cu, are mounted on the vacuum vessel. The major radius of the center of the vacuum vessel is 0.84 m. The whole machine is installed inside a bell-shaped vacuum vessel (i.e. a bell-jar) for thermal insulation. Extension ports connect between the plasma vacuum vessel and the bell-jar.

Plasma facing components consist of high Z materials only, i.e. a stainless steel vacuum vessel, 3 sets of molybdenum poloidal limiters and molybdenum divertor plates as shown in Fig. 2. The divertor plates are installed at the bottom of the vacuum vessel. The position of the surface of the divertor plates is the same as that of the poloidal limiter. The vacuum vessel is directly cooled by the water. Molybdenum plates for the poloidal limiter and the divertor are cooled via the

stainless steel supports cooled by the water. Note that low Z material is not utilized as a plasma facing component and low Z coating has never been carried out at all. The wall conditioning is carried out just before the experimental campaign. At first, extension ports are heated up to 110°C for 2 days. Electron cyclotron resonance discharge cleaning is carried out for the conditioning of the plasma facing components for 2 days, although the vacuum vessel cannot be heated to avoid the thermal load to the cryogenic system. It is effective for removing oxygen and carbon [14,15].

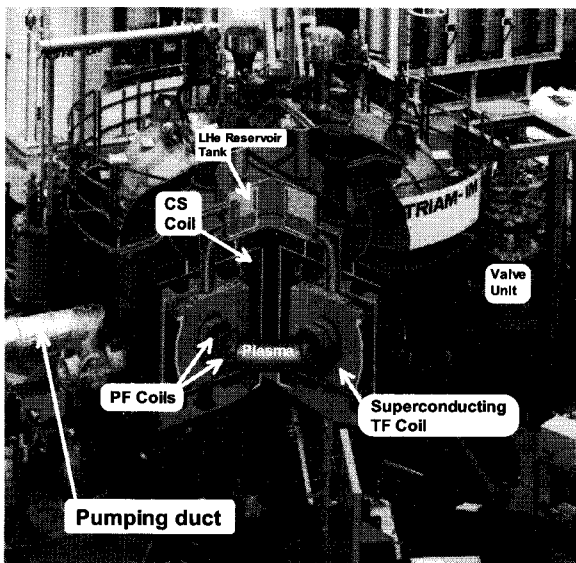


Fig. 1 Bird's eye view of TRIAM-1M.

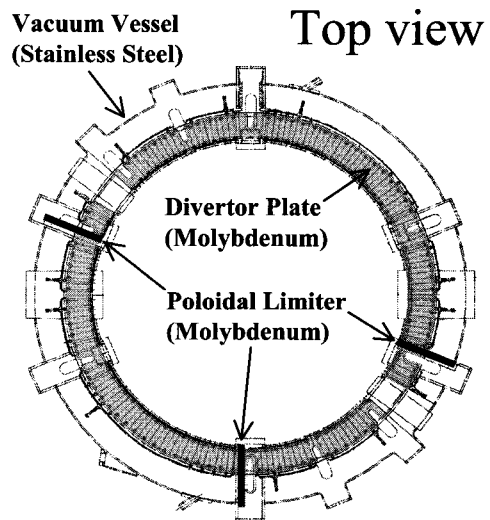
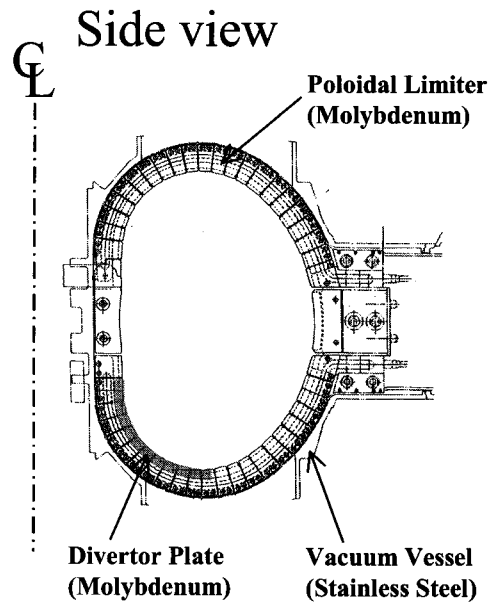


Fig. 2 Cross-sectional view of the plasma facing components.

Table 1 Parameters of the heating and current drive systems in TRIAM-1M.

| | Frequency (GHz) | Max. power (kW) | Pulse duration |
|------|-----------------|-----------------|----------------|
| LHCD | 2.45 | 50 | CW |
| | 8.2 | 200 | CW |
| | 8.2 | 200 | CW |
| ECH | 170 | 200 | 5 sec |

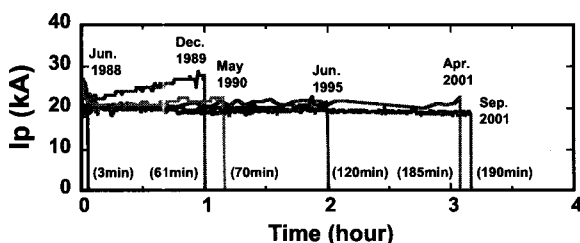


Fig. 3 Progress of the long tokamak operation in TRIAM-1M. The plasma current is sustained by 2.45 GHz lower hybrid current drive.

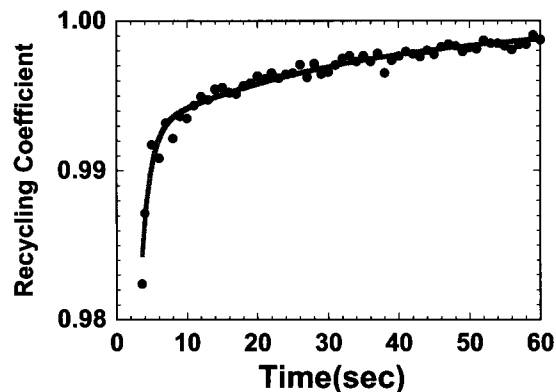
The heating and current drive systems in TRIAM-1M are summarized in Table 1. The ultra-long discharge of which the density range is less than about $0.2 \times 10^{19} \text{ m}^{-3}$ are sustained by the 2.45 GHz LHCD system. The high density and long duration discharges are sustained by the 8.2 GHz LHCD systems. Steady state and long duration discharges can be sustained by LHCD power alone.

Figure 3 shows the progress of the steady state tokamak operation in TRIAM-1M. It can be divided into 3 steps concerning from a viewpoint of the operation; the 3 min discharge (Jun. 1988), 1 hour discharges (Dec. 1989, May 1990) and longer than 2 hours (since 1995). In each step, the plasma position and fueling control systems were developed [6]. As far as the fueling control is concerned, the control system using the H_{α} line intensity has been developed. The gas feed is feedback controlled by a piezoelectric valve so as to keep the H_{α} line intensity at the central chord constant. The H_{α} line intensity is related with the number of hydrogen atoms that are ionized per unit time, i.e. particle influx to the plasma [16]. Thus the particle influx to the plasma is controlled during the discharge.

3. Experimental Results and Discussion

The particle balance equation inside the plasma is written by

$$dN_e/dt = \eta \Gamma_{\text{fuel}} + R N_e / \tau_p - N_e / \tau_p, \quad (1)$$

Fig. 4 Time evolution of the recycling coefficient of 2.45 GHz LHCD plasma. The line averaged electron density is about $0.2 \times 10^{19} \text{ m}^{-3}$.

where N_e is the total number of electrons in the plasma, η the fueling efficiency, Γ_{fuel} the fueling rate by the piezoelectric valve, R the recycling coefficient (i.e. the ratio of the hydrogen influx to the hydrogen out-flux on the plasma surface) and τ_p the particle confinement time. The value of the left hand side of eq. (1) can be obtained from the density profile measurement by the interferometer. The fueling efficiency η is obtained from the ratio of the increment of N_e to the total amount of the additional gas puff. The fueling rate is estimated from the voltage applied to the piezoelectric valve calibrated with the actual particle source rate. The sum of the first two terms of the right hand side of eq. (1) implies the influx of hydrogen atoms to the plasma and its amount is controlled by the piezoelectric valve. It can be evaluated from the radial profiles of the H_{α} line intensity and the electron density. Using eq. (1) and the value of $(\eta \Gamma_{\text{fuel}} + R N_e / \tau_p)$, two unknown parameters, R and τ_p , can be estimated. In eq. (1), the effect of impurity is not taken into account, namely, $Z_{\text{eff}} = 1$ is assumed. In the steady state condition (i.e., $dN_e/dt = 0$ and no impurity accumulation), however, the estimation of R from eq. (1) is considered to be valid, because the equation can be written by

$$\eta \Gamma_{\text{fuel}} + R \Gamma_{\text{out}} - \Gamma_{\text{out}} = 0, \quad (2)$$

where Γ_{out} is the hydrogen out-flux from the plasma and it is the same as the hydrogen influx.

The time evolution of the recycling coefficient in the steady state discharge is shown in Fig. 4. The recycling coefficient is rather high and increases with time. It means that the most of the hydrogen flux comes

from the wall, and the contribution of the external fueling (i.e., $\eta\Gamma_{\text{fuel}}$) decreases with time and it becomes $\sim 0.1\%$ of the total influx to the plasma at $t \sim 60$ s. Although the change of R in Fig. 4 is $\sim 2\%$, $\eta\Gamma_{\text{fuel}}$ decreases by a factor of twenty.

In this study, we note that the particle balance in the vacuum vessel. It can be written by

$$dN_{\text{H}}^0/dt + dN_{\text{H}}^p/dt = \Gamma_{\text{fuel}} - \Gamma_{\text{pump}} - \Gamma_{\text{wall}}, \quad (3)$$

where N_{H}^0 is the total number of hydrogen neutral atoms in the vessel, N_{H}^p the total number of hydrogen ions in the plasma, Γ_{pump} the pumping rate by the external pump-unit and Γ_{wall} the net wall pumping rate, which means the balance between the absorption rate and the release rate of the wall. Namely, Γ_{wall} is positive when the total number of hydrogen atoms absorbed by the wall is larger than that of hydrogen release from the wall. This means that the wall plays a role of the particle sink. When Γ_{wall} is negative, the wall plays a role of the particle source. From a viewpoint of the global particle balance, $\Gamma_{\text{wall}} = 0$ corresponds to be the apparent wall saturation. The first term of the left hand side of eq. (3) is deduced from the data of the ionization gauge at the pumping duct. N_{H}^p is assumed to be same as N_e . Γ_{pump} is the product of the neutral pressure and the pump speed of the external pump-unit at the ionization gauge. The unknown parameter Γ_{wall} can be obtained from the above equation.

Now, we will discuss about the particle balance in the longest discharge. The waveforms of the discharges are shown in Fig. 5. The plasma current was almost constant of ~ 20 kA during the discharge and was sustained by 2.45 GHz LHCD. The RF power decreased from 7.5 kW to 6.9 kW at $t \sim 46.6$ min to reduce the heat load to the limiter. Until $t \sim 30$ min, the H_{α} line intensity followed the reference level indicated by the chain line in Fig. 5 (b). The reference level was manually decreased about 6.5% at $t \sim 27$ min (denoted by an arrow) for the test of the wall condition. The H_{α} line intensity spontaneously increased around $t \sim 30$ min and reached to 1.6 times higher level. Moreover, the toroidal profile of the H_{α} line intensity was measured at four different positions (including a limiter position). All of the signals increased at the same rate after the apparent wall saturation. This suggests that the increase in the H_{α} line intensity (i.e. influx to the plasma) was caused by the contribution from the whole toroidal position. The OV and MoI line intensities were almost constant during the discharge as shown in Fig. 5 (c) and (d). Oxygen and Molybdenum are major impurities in

TRIAM-1M. Therefore, the wall seems to release the retained hydrogen. The piezoelectric valve automatically stopped fueling and afterwards did not supply the hydrogen gas at all until the end of the discharge. The time evolution of the neutral gas pressure at the pumping duct (Fig. 5 (e)) suggests that the neutral pressure in the main chamber also increased.

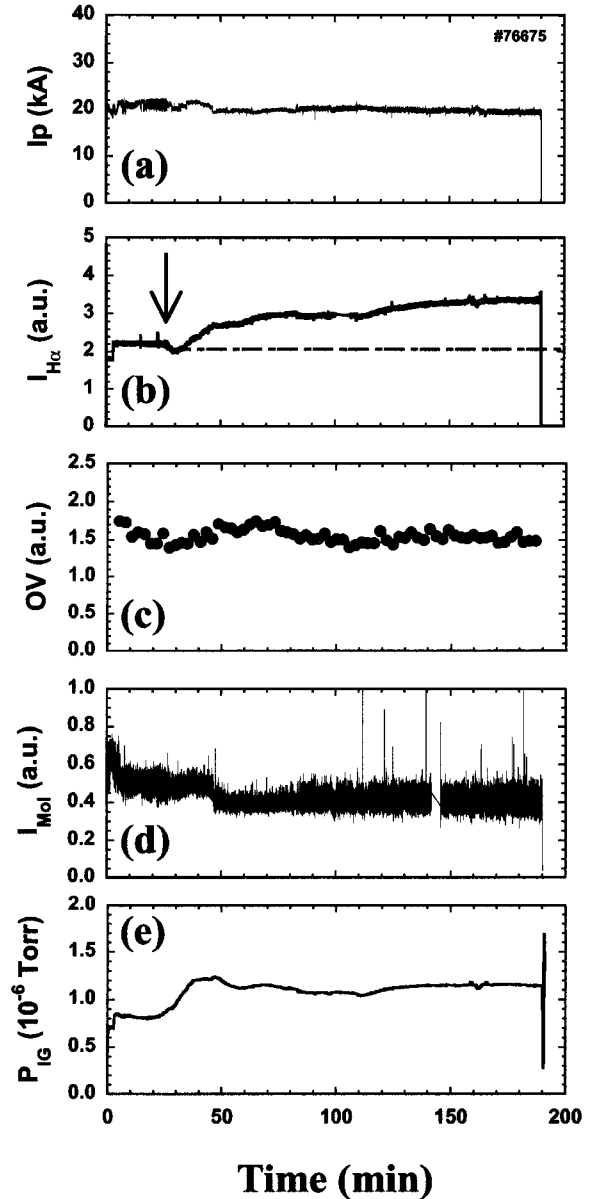


Fig. 5 Waveforms of the 3 hours discharge; (a) plasma current, (b) H_{α} line intensity (solid line) and reference level for the feedback control (chain line), (c) OV line intensity, (d) MoI line intensity and (e) neutral gas pressure at the pumping duct.

In the steady state condition, the wall pumping rate Γ_{wall} can be written by

$$\Gamma_{\text{wall}} = \Gamma_{\text{fuel}} - \Gamma_{\text{pump}} \quad (4)$$

since the two terms of the left hand side of eq. (3) is nearly zero and it seems to be no impurity accumulation. The averaged wall pumping rate from $t \sim 10$ to 20 min is estimated to be about 2.4×10^{16} atoms $\text{m}^{-2} \text{s}^{-1}$ from eq. (4). In this period, the wall played a role of the particle sink. The whole surface area ($S \sim 5 \text{ m}^2$) of the wall is used for the calculation of the wall pumping rate. After $t \sim 30$ min, $\Gamma_{\text{wall}} = -\Gamma_{\text{pump}} \sim -8 \times 10^{15}$ atoms $\text{m}^{-2} \text{s}^{-1}$, since the fueling was stopped ($\Gamma_{\text{fuel}} = 0$). In this period, the hydrogen release rate from the wall exceeded the absorption rate, therefore the wall played a role of the particle source and the recycling coefficient would be more than unity. The total number of hydrogen atoms supplied by the piezoelectric valve is estimated to be about 4×10^{20} . And the total number of hydrogen atoms pumped by the external pump-unit during the discharge is almost the same as that of the supplied hydrogen. Namely, it was observed that $\int \Gamma_{\text{fuel}} dt \sim \int \Gamma_{\text{pump}} dt$. From eq. (4), this means that the total amount of wall-pumped hydrogen atoms was finally released from the wall until the end of the discharge, i.e. $\int \Gamma_{\text{wall}} dt \sim 0$.

The detailed investigation of the mechanism of the apparent wall saturation during the discharge is a future work, but one candidate is the increase in the wall temperature, which is related to the out-gassing. The time evolution of the temperature of the plasma facing components is shown in Fig. 6. The temperature is measured by thermocouples. An infrared camera also measured the surface temperature of the interacting point between the plasma and the limiter plate. The

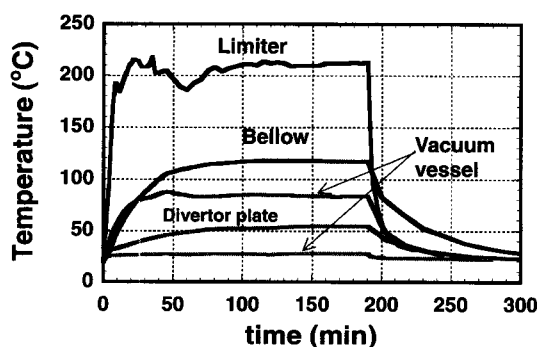


Fig. 6 Time evolution of the temperature of the limiter support, divertor plate and the vacuum vessel.

surface temperature also rapidly increased for 5 min and reached a quasi-steady state. The range of the surface temperature measured is about $600 \sim 800^\circ\text{C}$ provide that the emissivity ϵ of the molybdenum plate is unity. The real surface temperature is expected to be rather higher, since ϵ of the molybdenum plate seems to be low. The estimation of ϵ is a future work. The temperature and the characteristic time of the temperature increase, τ_T , depend on the balance between the heat load and the cooling ability, i.e. the distance of the measuring point from the cooling pipe. The value of τ_T is a few minutes for the limiter and a few tens of minute for the vacuum vessel and the divertor plate. It is considered that the limiter does not contribute the apparent wall saturation, since τ_T of the limiter is much less than the time of the apparent wall saturation t_s (~ 30 min). On the other hand, τ_T of the vacuum vessel is similar to t_s . Moreover, the increase in the H_α line intensity after the apparent wall saturation is considered to be caused by the overall contribution from the whole toroidal position as described above. So, one of causes of the apparent wall saturation in the longest discharge is considered to be the increase in the hydrogen release from the vacuum vessel due to the temperature increase.

4. Summary

In the superconducting tokamak TRIAM-1M, the longest discharge with the duration of longer than 3 hours was achieved. The global particle balance of this discharge was investigated. From the viewpoint of the global particle balance, the net wall pumping rate became zero around $t \sim 30$ min. After that the plasma was sustained without fueling until the end of the discharge. The averaged wall pumping rate is about 2.4×10^{16} atoms $\text{m}^{-2} \text{s}^{-1}$ before the apparent wall saturation and after that it becomes -8×10^{15} atoms $\text{m}^{-2} \text{s}^{-1}$. The wall plays both roles of the particle sink and the particle source. The total amount of wall-pumped hydrogen atoms was finally released from the wall until the end of the discharge. One of the causes of this apparent wall saturation is considered to be the increase in the hydrogen release from the wall due to the temperature increase.

Acknowledgement

This work is partly supported by a Grant-in-Aid for Scientific Research from the Ministry of Education, Culture, Sports, Science and Technology.

References

- [1] S. Itoh *et al.*, in *Plasma Phys. Contrl. Nucl. Fusion Research 1986 (Proc. 11th Int. Conf., Kyoto, 1986)* Vol.3, IAEA, Vienna, 321 (1987).
- [2] S. Itoh *et al.*, in *Plasma Phys. Contrl. Nucl. Fusion Research 1988 (Proc. 12th Int. Conf., Nice, 1988)* Vol.1, IAEA, Vienna, 629 (1989).
- [3] S. Itoh *et al.*, in *Plasma Phys. Contrl. Nucl. Fusion Research 1990 (Proc. 13th Int. Conf., Washington, DC, 1990)* Vol.1, IAEA, Vienna, 733 (1991).
- [4] S. Itoh *et al.*, in *Fusion Energy 1996 (Proc. 16th Int. Conf., Montreal, 1996)* Vol.3, IAEA, Vienna, 351 (1997).
- [5] M. Sakamoto *et al.*, *Proc. 24th EPS Conf. on Controlled Fusion and Plasma Physics, Berchtesgaden (European Physical Society, Geneva, 1997)* Vol. 21A, Part II, 351 (1997).
- [6] S. Itoh *et al.*, *Nucl. Fusion* **39**, 1257 (1999).
- [7] S. Itoh, *FURKU Report 01-04 (73)*, (2001) [*in Japanese*].
- [8] J. Jacquinet *et al.*, *Plasma Phys. Control. Fusion* **35**, A35 (1993).
- [9] Equipe Tore Supra (presented by F. Saint-Laurent), *Nucl. Fusion* **40**, 1047 (2000).
- [10] M. Sakamoto *et al.*, *Nucl. Fusion* **42**, 165 (2002).
- [11] T. Hirai *et al.*, *J. Nucl. Mater.* **258-268**, 1060 (1998).
- [12] R. Behrisch *et al.*, *J. Nucl. Mater.* **233-237**, 673 (1996).
- [13] T. Hirai *et al.*, *J. Plasma Fusion Res. SERIES 3*, 284 (2000).
- [14] E. Jotaki and S. Itoh, *Fusion Eng. Des.* **36**, 447 (1997).
- [15] K. Hanada *et al.*, *Fusion Eng. Des.* **54**, 79 (2001).
- [16] G.M. McCracken *et al.*, *Nucl. Fusion* **18**, 35 (1978).